Induction of apoptosis and inhibition of cyclooxygenase-2 expression by *N*-methyl-*N*′-nitro-*N*-nitrosoguanidine in human leukemia cells

Cheol Park[a], Byung Tae Choi[b,c], Kwang Il Kang[d], Taeg Kyu Kwon[e], Jaehun Cheong[f], Won Ho Lee[g], Nam Deuk Kim[h] and Yung Hyun Choi[a,c]

Previous studies have demonstrated that *N*-methyl-*N*′-nitro-*N*-nitrosoguanidine (MNNG), a well-known DNA alkylating agent, induces G_2/M arrest and apoptotic cell death in several human cancer cell lines. In the present study, we investigated the effects of MNNG on the growth of a U937 human leukemia cell model. The effects of this compound were also tested on cyclooxygenase (COX) activity. Treatment of U937 cells with MNNG resulted in the inhibition of viability and the induction of apoptosis in a concentration-dependent manner, which was associated with a dose-dependent upregulation in pro-apoptotic Bax protein, downregulation of anti-apoptotic Bcl-2 and Bcl-x_L proteins, and proteolytic activation of caspase-3 protease. Furthermore, MNNG decreased the levels of COX-2 mRNA and protein expression without significant changes in the levels of COX-1, which was correlated with inactivation of the reporter construct of a COX-2 promoter and decrease in prostaglandin E_2 synthesis. Taken together, these findings provide important new insights into the possible molecular mechanisms of the anti-cancer activity of MNNG. *Anti-Cancer Drugs* **16:507–513 © 2005 Lippincott Williams & Wilkins.**

Anti-Cancer Drugs 2005, **16**:507–513

Keywords: apoptosis, Bax, cyclooxygenase, *N*-methyl-*N*′-nitro-*N*-nitrosoguanidine

Departments of [a]Biochemistry and, [b]Anatomy, Dongeui University College of Oriental Medicine, [c]Department of Biomaterial Control, Dongeui University Graduate School, Busan 614-052, South Korea, [d]Institute of Biotechnology, Chungnam National University, Daejeon 305-764, South Korea, [e]Department of Immunology, School of Medicine, Keimyung University, Taegu 700-712, South Korea and Departments of [f]Molecular Biology, [g]Biology and [h]Pharmacy and Pusan Cancer Research Center, Pusan National University, Busan 609-735, South Korea.

Sponsorship: This work was supported by Korea Research Foundation Grant to Y. H. C. (KRF-2002-041-E00024) and Pusan National University Research Grant to N. D. K.

Correspondence to Y. H. Choi, Department of Biochemistry, Dongeui University College of Oriental Medicine, Busan 614-052, South Korea.
Tel: +82 51 857413; fax: +82 51 853 4036;
e-mail: choiyh@deu.ac.kr

Received 9 November 2004 **Revised form accepted** 23 February 2005

Introduction

It has been suggested that non-steroidal anti-inflammatory drugs (NSAIDs) reduce the risk of cancer and that the inhibition of carcinogenesis by NSAIDs is mediated through the modulation of prostaglandin production from the substrate arachidonic acid by rate-limiting enzymes known as cyclooxygenases (COXs) [1,2]. Prostaglandins are lipid mediators that are involved in many normal physiological processes, and are implicated in many pathological processes including inflammation, edema, fever, hyperalgesia, cancer and Alzheimer's disease. Two distinct COXs have been identified: COX-1, which is constitutively expressed, and COX-2, which is induced by different products such as tumor promoters or growth factors [3–6]. Overexpression of COX-2 has been observed in most cancer cell species [7,8]; therefore, specific inhibitors of COX-2 could serve as chemopreventive and/or therapeutic agents.

Genotoxic events can activate various signaling pathways that serve, for example, to activate DNA repair mechanisms, halt cell cycle progression and/or trigger advancement into apoptotic cell death. Although all genotoxins produce such general responses, the mechanisms that govern the response to divergent forms of DNA damage are potentially diverse themselves. *N*-Methyl-*N*′-nitro-*N*-nitrosoguanidine (MNNG), an alkylating agent inducing O^6-methyluanine in DNA, is not only highly mutagenic and carcinogenic, but also very cytotoxic because of the induction of apoptosis [9,10]. MNNG is known to cause growth arrest at the G_2/M checkpoint and apoptosis in various types of cell lines, including human cancer cells [11–20]. Previous reports showed that the treatment of human cancer cells with MNNG results in p53 phosphorylation on serine residues and these phosphorylation events depend on the presence of functional protein complexes involved in mismatch repair [21–23]. These results implicate action of the mismatch repair system in the initial step of a damage-signaling cascade that can lead to cell-cycle checkpoint activation or apoptosis in response to DNA damage [22–24]. Additionally, it has been shown that the Jun-N-terminal kinase/stress-activated protein kinases and p38 kinase are activated in MNNG-treated cells [25]. To date, despite accumulated

0959-4973

data, the precise molecular mechanism by which MNNG induces apoptosis is poorly understood.

In this study, to elucidate the further mechanisms of MNNG-induced growth inhibition of the cancer cells, we investigated the effect of MNNG on the induction of apoptosis in the human leukemia U937 cell line. Moreover, the effects of this compound were tested on COX expression and activity.

Materials and methods

Cell culture and viability study

The human leukemia cell line U937 was purchased from the ATCC (Rockville, MD), and cultured in RPMI 1640 medium supplemented with 10% heat-inactivated fetal calf serum (FCS), 2 mM L-glutamine, 100 μg/ml streptomycin and 100 μg/ml penicillin at 37°C and 5% CO_2.. MNNG was purchased from Sigma (St Louis, MO), dissolved in distilled water. For the viability study, cells were cultured in the absence and presence of variable concentrations of MNNG for 48 h. The cells were washed with phosphate-buffered saline (PBS) and the viable cells were scored with a hemocytometer through the exclusion of Trypan blue.

Nuclear staining with 4,6-diamidino-2-phenylindile (DAPI)

Cells were washed with cold PBS and fixed with 3.7% paraformaldehyde (Sigma) in PBS for 10 min at room temperature. Fixed cells were washed with PBS and stained with DAPI (Sigma) solution for 10 min at room temperature. The cells were washed a further 2 times with PBS and analyzed via a fluorescent microscope.

Flow cytometric analysis

Cells were washed with PBS, pelleted by low-speed centrifugation, resuspended in citrate buffer and treated with RNase A as previously described [26]. Nuclei were stained with a propidium iodide (PI; Sigma) solution. The DNA content in each cell nucleus was determined by a FACScan flow cytometer (Becton Dickinson, San Jose, CA).

DNA fragmentation assay

After treatment with MNNG, cells were lysed in a buffer containing 10 mM Tris–HCl (pH 7.4), 150 mM NaCl, 5 mM EDTA and 0.5% Triton X-100 for 30 min on ice. Lysates were vortexed and cleared by centrifugation at 10 000 *g* for 20 min. Fragmented DNA in the supernatant was extracted with an equal volume of neutral phenol: chloroform:isoamylalcohol (25:24:1, v/v/v) and analyzed electrophoretically on 1% agarose gel containing 0.1 μg/ml ethidium bromide (EtBr).

RNA extraction and RT-PCR

Total RNA was isolated according to the previously published method [27]. Single-strand cDNA was synthesized from 2 μg of total RNA using M-MLV reverse transcriptase (Gibco/BRL, Gaithersburg, MD). The mRNAs were amplified by polymerase chain reaction (PCR) with primers indicated in Table 1. Conditions for the PCR reaction were 1 × (94°C, 3 min), 35 × (94°C, 45 s; 58°C, 45 s; 72°C, 1 min) and 1 × (72°C, 10 min). Amplification products obtained by PCR were electrophoretically separated on 1% agarose gel.

Table 1 Oligonucleotides used in RT-PCR

Name		Sequence of primers
Bax	sense	5′-ATG GAC GGG TCC GGG GAG-3′
	antisense	5′-TGG AAG AAG ATG GGC TGA-3′
Bcl-2	sense	5′-CAG CTG CAC CTG ACG-3′
	antisense	5′-GCT GGG TAG GTG CAT-3′
Bcl-x_L	sense	5′-CAG CTG CAC CTG ACG-3′
	antisense	5′-GCT GGG TAG GTG CAT-3′
Caspase-3	sense	5′-ATG GAG AAC ACT GAA AAC TCA-3′
	antisense	5′-GAA CTC TAT TTT TAT CAC TAA-3′
COX-1	sense	5′-TGC CCA GCT CCT GGC CCG CCG CTT-3′
	antisense	5′-GTG CAT CAA CAC AGG CGC CTC TTC-3′
COX-2	sense	5′-TTC AAA TGA GAT TGT GGG AAA AT-3′
	antisense	5′-AGA TCA TCT CTG CCT GAG TAT CTT-3′
GAPDH	sense	5′-CGG AGT CAA CGG ATT TGG TCG TAT-3′
	antisense	5′-AGC CTT CTC CAT GGT GGT GAA GAC-3′

Gel electrophoresis and Western blot analysis

The cells were harvested, lysed and protein concentrations were quantified using the Bio-Rad protein assay (Bio-Rad, Hercules, CA), following the procedure described by the manufacturer. Western blot analysis was performed as described [28]. Briefly, an equal amount of protein was subjected to electrophoresis on SDS–polyacrylamide gels and transferred to nitrocellulose membranes (Schleicher & Schuell, Keene, NH) by electroblotting. Blots were probed with the desired antibodies for 1 h, incubated with diluted enzyme-linked secondary antibody and then visualized by the enhanced chemiluminescence (ECL) according to the recommended procedure (Amersham, Arlington Heights, IL). The primary antibodies were purchased from Santa Cruz Biotechnology (Santa Cruz, CA). Peroxidase-labeled donkey anti-rabbit immunoglobulin and peroxidase-labeled sheep anti-mouse immunoglobulin were purchased from Amersham.

Caspase-3 protease activity assay

Caspase-3 activity was assayed by cleavage of Asp-Glu-Val-Asp (DEVD)-*p*-nitroanilide (pNA) using a commercially available kit (Clontech, Palo Alto, CA). Briefly, cells were cultured in the presence or absence of MNNG and then 2×10^6 cells were incubated with DEVD-pNA in the presence of dithiothreitol for 60 min at 37°C. The reaction was measured by changes in absorbance at 405 nm using the VERSAmax tunable microplate reader (Molecular devices, Palo Alto, CA).

Prostaglandin E_2 (PGE_2) enzyme immunoassay (EIA) analysis

Cells were plated on 10-cm diameter plates at 6×10^5 cells/plate and allowed to adhere overnight. After treating with MNNG, the medium was removed and PGE_2 production by cells was measured. To measure the PGE_2 accumulation, EIA was performed using a commercial kit (Cayman Chemicals, Ann Arbor, MI) according to the manufacturer's protocol. PGE_2 production was normalized with respect to the number of viable cells present in the particular culture.

Transfections and luciferase assay

To measure COX-2 transcriptional activation, cells were transiently co-transfected with the full-length human COX-2 promoter–luciferase reporter construct (kindly provided by Professor T. K. Kwon, Department of Immunology, Keimyung University School of Medicine, Taegu, South Korea) and with the β-galactosidase reporter vector pCMBβ (Promega, Madison, WI) using LipofectAMINE transfection reagent (Gibco/BRL), according to the manufacturer's recommendations. Following transfection, the cells were incubated for 12 h, the medium was exchanged and the cells were incubated for an additional 36 h in the presence or absence of MNNG. The cells were then lysed and luciferase activity in the lysates was assayed using a Dynatech ML1000 luminometer (Dynatech, Chantilly, VA) as previously described [26]. Luciferase activity was normalized to β-galactosidase activity, which was assayed using the β-galactosidase enzyme assay system (Promega).

Results and discussion

Inhibition of the viability and induction of apoptosis by MNNG

Cells were cultured in 10% FCS-containing medium with or without MNNG (0.02–0.1 μg/ml) during 48 h and cell viability was evaluated. As shown in Fig 1(A), MNNG had a marked dose-dependent inhibitory effect on U937 cell viability. The viability was inhibited by more than 45 or 70% in cells exposed to 0.04 or 0.1 μg/ml MNNG, respectively, as compared to untreated control cells. We then examined whether this inhibitory effect of MNNG on cell growth was a result of apoptotic cell death. By morphological analysis with DAPI staining, the untreated control cells displayed intact nuclear structures, while cells treated with MNNG had chromosomal condensation and the formation of apoptotic bodies, characteristics of apoptosis [29,30], in a concentration-dependent manner, indicating MNNG induced apoptotic cell death (Fig. 1B).

Another hallmark of apoptosis is a degradation of chromosomal DNA at internucleosomal linkages [30,31]. Accordingly, we analyzed whether DNA fragmentation was induced by MNNG in U937 cells. Following agarose gel electrophoresis of U937 cells treated with 0.05 and 0.1 μg/ml MNNG for 48 h, a typical ladder pattern of internucleosomal fragmentation was observed (Fig. 2A). To quantify the degree of apoptosis, we analyzed the amount of sub-G_1 DNA by flow cytometry of fixed nuclei. As shown in Fig. 2(B), the addition of MNNG to U937 cells resulted in markedly increased accumulation of the sub-G_1 phase in a dose-dependent manner. These results suggest that, following

Fig. 1

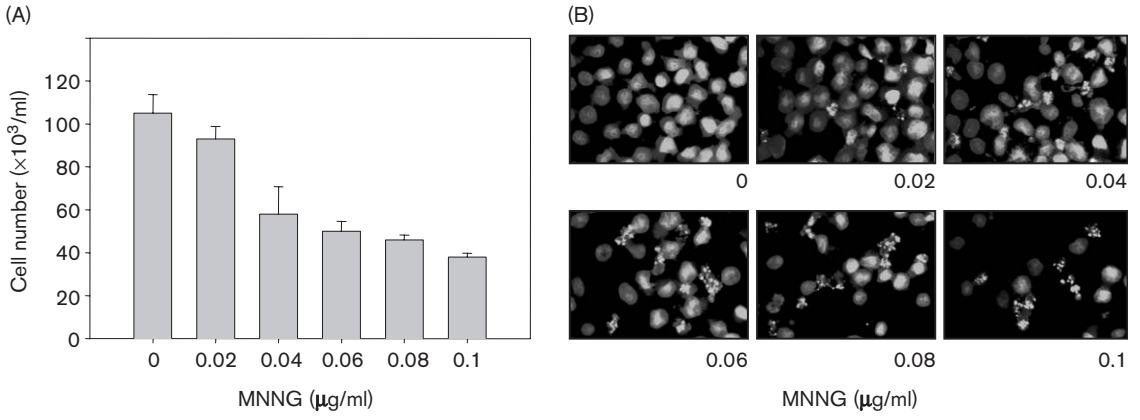

Effects of MNNG on the viability and morphology of U937 cells. (A) Cells were seeded at 3×10^4/ml in 35-mm dishes and incubated for 24 h. The cells were cultured in the absence (0, control) or in the presence of increasing concentrations of MNNG for 48 h. Viable cell number was determined by hemocytometer counts of Trypan blue-excluding cells. The results are expressed as the mean ± SD of data from three separate experiments. (B) Cells were incubated with MNNG for 48 h and then stained with DAPI. After a 10-min incubation at room temperature, the cells were washed with PBS and photographed with a fluorescence microscope using a blue filter. Magnification × 400.

MNNG treatment, U937 cells accomplish apoptosis, and that there is a good correspondence between the extent of apoptosis and growth inhibition.

Induction of Bax and activation of caspase-3 by MNNG

Apoptotic cell death is highly regulated by pro- and anti-apoptotic modulators, including members of the Bcl-2 family [32,33]. To analyze whether MNNG induces cell death by modulating the expression of Bcl-2 family members, after exposure to different concentrations of MNNG, total RNAs and cellular proteins were isolated, and immunoblotting and RT-PCR were performed. As shown in Fig. 3, the levels of protein and mRNA of Bax, a pro-apoptotic gene, were markedly induced in MNNG-treated cells. However, MNNG did not affect the levels of Bcl-2 and Bcl-x_L mRNA, anti-apoptotic genes, whereas the protein levels of Bcl-2 and Bcl-x_L were significantly inhibited in response to MNNG treatment in a concentration-dependent fashion. Our data indicated that the apoptotic effects of MNNG on U937 cells are partly caused by upregulating the Bax/Bcl-2 or Bcl-x_L protein ratio, which is a critical determinant of apoptosis.

Fig. 2

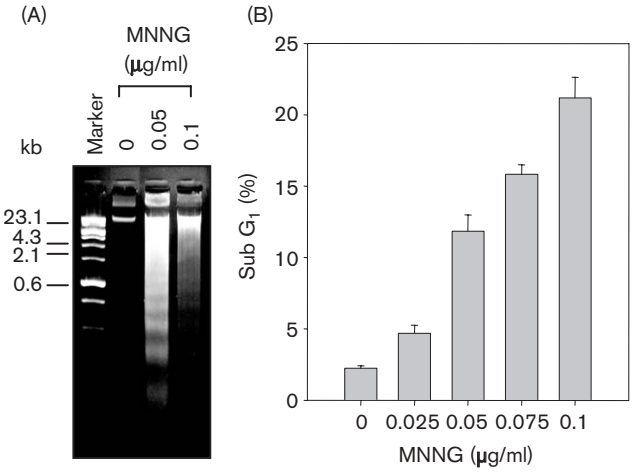

Induction of DNA fragmentation and increase of sub-G_1 population by MNNG in U937 cells. (A) To analyze fragmentation of genomic DNA, cells were treated for 48 h with the indicated concentrations of MNNG. Fragmented DNA was extracted and analyzed on 1% agarose gel. (B) Cells were treated for 48 h with MNNG and evaluated for DNA content after PI staining. The fraction of apoptotic sub-G_1 cells is indicated. The results are expressed as the mean ± SD of data from three separate experiments.

Recent studies have identified caspases as important mediators of apoptosis induced by various apoptotic stimuli [34,35]. To determine the roles of caspases in MNNG-induced apoptosis, we measured the expression levels and *in vitro* activities of caspase-3 in U937 cells treated with MNNG, which is activated by proteolytic processing of the 32-kDa form into two smaller subunits [34,35]. As shown in Fig. 4(A and B), RT-PCR and immunoblotting data indicated that MNNG did not affect the expression of caspase-3 mRNA and pro-caspase-3 protein. However, the active subunits of the caspase-3 form were concentration-dependently increased by MNNG treatment. To further quantify the proteolytic activity of caspase-3 by MNNG, we performed an *in vitro* assay using a fluorogenic substrate specific for caspase-3, DEVD-pNA. U937 cells displayed 3.2- and 4.1-fold increases in DEVD-pNA cleavage after a 48-h exposure to 0.075 and 0.1 μg/ml MNNG, respectively (Fig. 4B). These results suggest that MNNG-induced apoptosis in U937 cells is mediated, at least in part, by the mitochondrial-signaling pathway.

Fig. 3

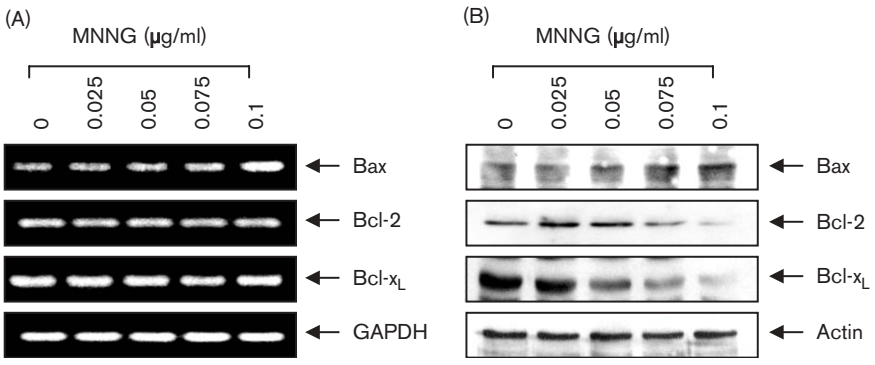

Effects of MNNG on Bcl-2 family expression. (A) After a 48-h incubation with MNNG, total RNAs were isolated and reverse transcribed. The resulting cDNAs were subjected to PCR with the indicated primers, and the reaction products were subjected to electrophoresis in a 1% agarose gel and visualized by EtBr staining. GAPDH was used as an internal control. (B) The cells were lysed, and then cellular proteins were separated by SDS–PAGE and transferred onto nitrocellulose membranes. The membranes were probed with the indicated antibodies. Proteins were visualized using an ECL detection system. Actin was used as an internal control.

Fig. 4

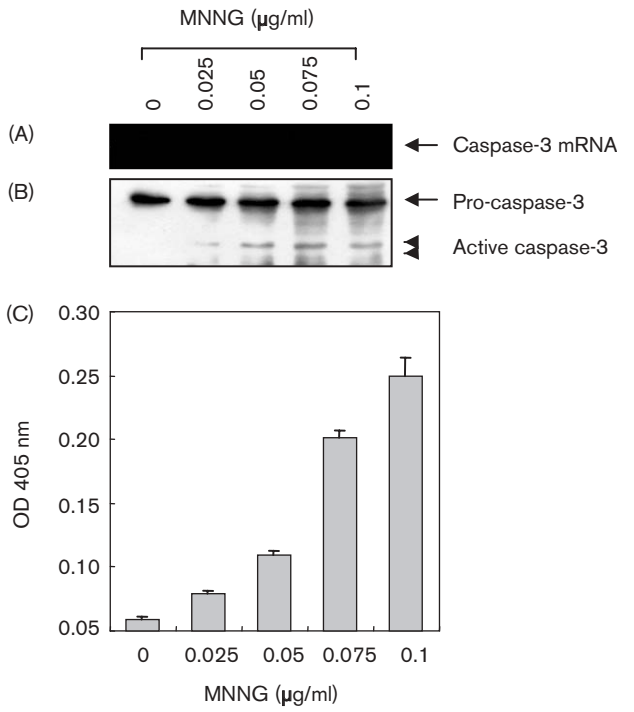

Proteolytic activation of caspase-3 by MNNG in U937 cells. (A) After a 48-h incubation with MNNG, total RNAs were isolated and reverse transcribed. The resulting cDNAs were subjected to PCR with the caspase-3 primer, and the amplified PCR products were subjected to electrophoresis in a 1% agarose gel and visualized by EtBr staining. (B) Cells were treated with the indicated concentrations of MNNG for 48 h and collected. The cells were lysed and then cellular proteins were separated by 13% SDS–PAGE and transferred onto a nitrocellulose membrane. The membrane was probed with the antibody against caspase-3 and visualized using an ECL detection system. (C) Aliquots (50 μg protein) were incubated with DEVD-pNA for *in vitro* caspase-3 activity at 37°C for 1 h. The released fluorescent products were measured using an ELISA reader. The results are expressed as the mean ± SD of data from three separate experiments.

Inhibition of COX-2 expression and PGE_2 accumulation by MNNG

In a number of experimental studies, induction of COX-2, the enzyme catalyzing the rate-limiting step in prostaglandin biosynthesis from the substrate arachidonic acid, has been shown to promote cell growth, inhibit apoptosis and enhance cell motility [2,36,37]. Moreover, compelling evidence from genetic and clinical studies indicates that COX-2 upregulation is a key step in carcinogenesis, and there is a clear positive correlation between COX-2 expression and inhibition of apoptosis. Overexpression of COX-2 is sufficient to cause tumorigenesis in animal models, and inhibition of the COX-2 pathway results in reduction in tumor incidence and progression [37,38]. Therefore, inhibition of COX-2 activity promises to be an effective approach in the prevention and treatment of cancer. To determine whether MNNG reduces expression of COXs and production of PGE_2 in U937 cells, the cells were treated with MNNG for 48 h. In our study, RT-PCR and Western blot analyses showed a significant decrease in COX-2 mRNA and protein expression over time after MNNG treatment, but MNNG was ineffective on COX-1 (non-inducible form) expression (Fig. 5). To confirm that PGE_2 production was associated with the catalytic activity of the COX-2 isoform, U937 cells were cultured in the presence of MNNG and PGE_2 levels were measured. As shown in Fig. 6(A), the synthesis of PGE_2 was concentration dependent and this production was significantly decreased over time after MNNG treatment, which was well correlated with downregulation of COX-2 expression. Since the COX-2 expression is markedly inhibited by MNNG, we subsequently investigated the effect of MNNG on the promoter activity of COX-2, using the COX-2 luciferase reporter that contains a luciferase gene under the control of a full-length COX-2 promoter. As shown in Fig. 6(B), following exposure to MNNG, the COX-2 promoter construct was significantly

Fig. 5

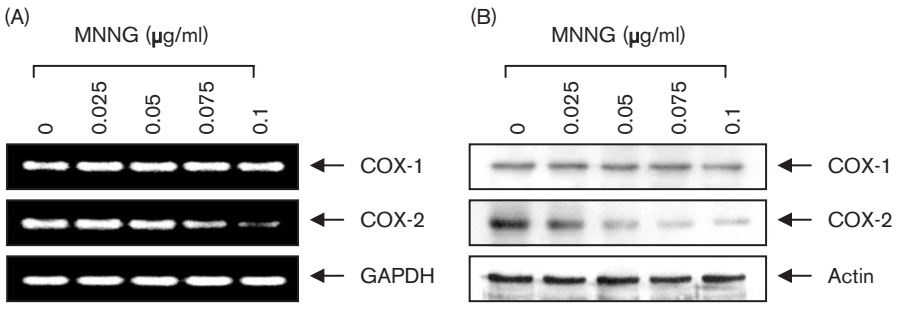

Downregulation of COX-2 expression by MNNG in U937 cells. (A) After a 48-h incubation with MNNG, total RNAs were isolated and reverse transcribed. The resulting cDNAs were subjected to PCR with COX-1 and -2 primers, and the reaction products were subjected to electrophoresis on a 1% agarose gel and visualized by EtBr staining. GAPDH was used as an internal control. (B) Cells were treated with the indicated concentrations of MNNG for 48 h and collected. The cells were lysed and then cellular proteins were separated by 10% SDS–PAGE and transferred onto nitrocellulose membranes. The membranes were probed with the antibodies against COX-1, COX-2 and actin. Proteins were visualized using an ECL detection system. Actin was used as an internal control.

Fig. 6

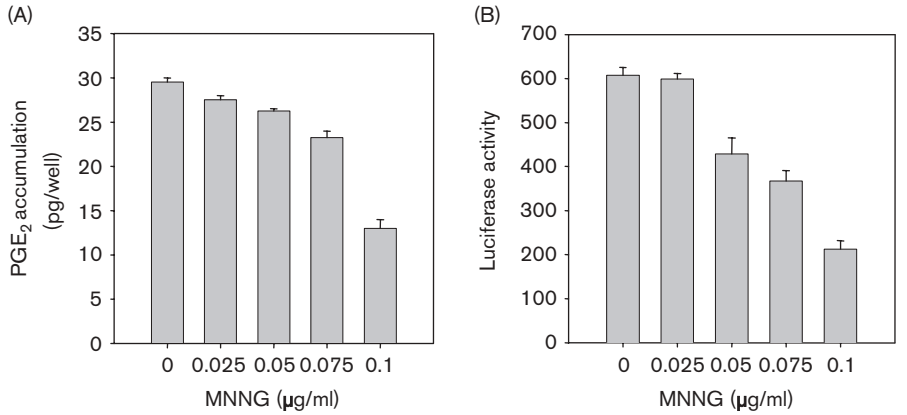

Inhibition of PGE_2 production and COX-2 promoter–luciferase fusion plasmid activity in U937 cells after exposure to MNNG. (A) Cells were treated with the indicated concentrations of MNNG for 48 h and collected. The PGE_2 accumulation in the medium was determined by an EIA kit as described in Materials and methods. The results are expressed as the mean ± SD of data from two separate experiments. (B) The COX-2 promoter construct fused to the luciferase gene and the β-galactosidase reporter vectors were transiently co-transfected into cells. The cells were treated with different concentrations of MNNG; luciferase activities, which were normalized to the β-galactosidase enzyme assay system, are expressed as fold increase from control. The results are expressed as the mean ± SD of data from three separate experiments.

inactivated in a concentration-dependent manner. The data suggested that the inhibition of the COX-2 expression and PGE_2 production is consistent with the results that MNNG inhibited the growth and induced apoptosis.

In conclusion, our results suggest that MNNG induces an inhibition of human leukemia U937 cell growth with an apoptosis induction. The apoptotic events were mediated by an increase in Bax expression and an activation of caspase-3 protease. The growth inhibitory effects of MNNG were also associated with a specific inhibition of COX-2 activity. These novel phenomena have not been previously described and provide important new insights into the possible biological effects of MNNG. However, our study does not reveal a clear relationship between Bcl-2 and COX-2 to induce apoptosis, and future work in our laboratory will seek to understand the precise molecular mechanism(s) of MNNG's action.

References

1 Anderson WF, Umar A, Viner JL, Hawk ET. The role of cyclooxygenase inhibitors in cancer prevention. *Curr Pharm Des* 2002; **8**:1035–1062.

2 Soh JW, Weinstein IB. Role of COX-independent targets of NSAIDs and related compounds in cancer prevention and treatment. *Prog Exp Tumor Res* 2003; **37**:261–285.

3 Smith WL, Garavito RM, DeWitt DL. Prostaglandin endoperoxide H synthases (cyclooxygenases)-1 and -2. *J Biol Chem* 1996; **271**: 33157–33160.

4 Smith WL, DeWitt DL, Garavito RM. Cyclooxygenases: structural, cellular, and molecular biology. *Annu Rev Biochem* 2000; 69;145–182.

5 Tao X, Schulze-Koops H, Ma L, Cai J, Mao Y, Lipsky PE. Effects of *Tripterygium wilfordii* hook F extracts on induction of cyclooxygenase 2 activity and prostaglandin E_2 production. *Arthritis Rheum* 1998; **41**: 130–138.

6 Repovic P, Mi K, Benveniste EN, Oncostatin M. enhances the expression of prostaglandin E_2 and cyclooxygenase-2 in astrocytes: synergy with interleukin-1β, tumor necrosis factor-alpha, and bacterial lipopolysaccharide. *Glia* 2003; **42**:433–446.

7 Crofford LJ. COX-1 and COX-2 tissue expression: implications and predictions. *J Rheumatol* 1997; **49**(**suppl**):15–19.

8 Cao Y, Prescott SM. Many actions of cyclooxygenase-2 in cellular dynamics and in cancer. *J Cell Physiol* 2002; **190**:279–286.

9 Beranek DT. Distribution of methyl and ethyl adducts following alkylation with monofunctional alkylating agents. *Mutat Res* 1990; **231**:11–30.

10 Edara S, Kanugula S, Pegg AE. Expression of the inactive C145A mutant human O^6-alkylguanine-DNA alkyltransferase in *E. coli* increases cell killing and mutations by *N*-methyl-*N*′-nitro-*N*-nitrosoguanidine. *Carcinogenesis* 1999; **20**:103–108.

11 Hawn MT, Umar A, Carethers JM, Marra G, Kunkel TA, Boland CR, *et al.* Evidence for a connection between the mismatch repair system and the G_2 cell cycle checkpoint. *Cancer Res* 1995; **55**:3721–3725.

12 Carethers JM, Hawn MT, Chauhan DP, Luce MC, Marra G, Koi M, *et al.* Competency in mismatch repair prohibits clonal expansion of cancer cells treated with *N*-methyl-*N*′-nitro-*N*-nitrosoguanidine. *J Clin Invest* 1996; **98**:199–206.

13 Hour TC, Shiau SY, Lin JK. Suppression of *N*-methyl-*N*′-nitro-*N*-nitrosoguanidine- and *S*-nitrosoglutathione-induced apoptosis by Bcl-2 through inhibiting glutathione-S-transferase pi in NIH3T3 cells. *Toxicol Lett* 1999; **110**:191–202.

14 Khan QA, Dipple A. Diverse chemical carcinogens fail to induce G_1 arrest in MCF-7 cells. *Carcinogenesis* 2000; **21**:1611–1618.

15 Rasmussen LJ, Rasmussen M, Lutzen A, Bisgaard HC, Singh KK. The human cyclin B1 protein modulates sensitivity of DNA mismatch repair deficient prostate cancer cell lines to alkylating agents. *Exp Cell Res* 2000; **257**:127–134.

16 Fang MZ, Lee MH, Lee YS, Kim YC, Lee BM, Cho MH. Low expression of cyclin D2 in G_2/M-arrested and transformed proliferating Balb/3T3 cells. *J Vet Med Sci* 2001; **64**:201–205.

17 Fang MZ, Mar WC, Cho MH. Cell cycle was disturbed in the MNNG-induced initiation stage during *in vitro* two-stage transformation of Balb/3T3 cells. *Toxicology* 2001; **163**:175–184.

18 Cejka P, Stojic L, Mojas N, Russell AM, Heinimann K, Cannavo E, *et al.* Methylation-induced G_2/M arrest requires a full complement of the mismatch repair protein hMLH1. *EMBO J* 2003; **22**:2245–2254.

19 Dunkern T, Roos W, Kaina B. Apoptosis induced by MNNG in human TK6 lymphoblastoid cells is p52 and Fas/CD95/Apo-1 related. *Mutat Res* 2003; **544**:167–172.

20 Park C, Choi BT, Cheong J, Moon SK, Kim CH, Lee WH, *et al.* Induction of apoptosis and G_2/M arrest by *N*-methyl-*N*′-nitro-*N*-nitrosoguanidine in human prostate carcinoma cells. *Mutat Res* 2004; **563**:139–149.

21 Duckett DR, Bronstein SM, Taya Y, Modrich P. hMutSα- and hMutLα-dependent phosphorylation of p53 in response to DNA methylator damage. *Proc Natl Acad Sci USA* 1996; **96**:12384–12388.

22 Hickman MJ, Samson LD. Role of DNA mismatch repair and p53 in signaling induction of apoptosis by alkylating agents. *Proc Natl Acad Sci USA* 1999; **96**:10764–10769.

23 Adamson AW, Kim WJ, Shangary S, Baskaran R, Brown KD. ATM is activated in response to *N*-methyl-*N*′-nitro-*N*-nitrosoguanidine-induced DNA alkylation. *J Biol Chem* 2002; **277**:38222–38229.

24 Jaiswal AS, Narayan S. SN2 DNA-alkylating agent-induced phosphorylation of p53 and activation of p21 gene expression. *Mutat Res* 2002; **500**:17–30.

25 Wilhelm D, Bender K, Knebel A, Angel P. The level of intracellular glutathione is a key regulator for the induction of stress-activated signal transduction pathways including Jun N-terminal protein kinases and p38 kinase by alkylating agents. *Mol Cell Biol* 1997; **17**:4792–4800.

26 Choi YH, Lee WH, Park KY, Zhang L. p53-independent induction of p21 (WAF1/CIP1), reduction of cyclin B1 and G_2/M arrest by the isoflavone genistein in human prostate carcinoma cells. *Jpn J Cancer Res* 2000; **91**:164–173.

27 Choi YH, Kong KR, Kim YA, Jung KO, Kil JH, Rhee SH, *et al.* Induction of Bax and activation of caspases during β-sitosterol-mediated apoptosis in human colon cancer cells. *Int J Oncol* 2003; **23**:1657–1661.

28 Choi YH, Lee SJ, Nguyen P, Jang JS, Lee J, Wu ML, *et al.* Regulation of cyclin D1 by calpain protease. *J Biol Chem* 1997; **272**:28479–28484.

29 Gerschenson LE, Rotello RJ. Apoptosis: a different type of cell death. *FASEB J* 1992; **6**:2450–2455.

30 Saraste A. Morphologic criteria and detection of apoptosis. *Herz* 1999; **24**:189–195.

31 Walker PR, Sikorska M. New aspects of the mechanism of DNA fragmentation in apoptosis. *Biochem Cell Biol* 1997; **75**:287–299.

32 Miyashita T, Krajewski S, Krajewska M, Wang HG, Lin HK, Liebermann DA, *et al.* Tumor suppressor p53 is a regulator of *bcl-2* and *bax* gene expression *in vitro* and *in vivo*. *Oncogene* 1994; **9**:1799–1805.

33 Rosse T, Olivier R, Monney L, Rager M, Conus S, Fellay I, *et al.* Bcl-2 prolongs cell survival after Bax-induced release of cytochrome *c*. *Nature* 1998; **391**:496–499.

34 Stennicke HR, Salvesen GS. Properties of the caspases. *Biochim Biophys Acta* 1998; **1387**:17–31.

35 Earnshaw WC, Martins LM, Kaufmann SH. Mammalian caspases: structure, activation, substrates, and functions during apoptosis. *Annu Rev Biochem* 1999; **68**:383–424.

36 Dempke W, Rie C, Grothey A, Schmoll HJ. Cyclooxygenase-2: a novel target for cancer chemotherapy? *J Cancer Res Clin Oncol* 2001; **127**:411–417.

37 Gately S, Kerbel R. Therapeutic potential of selective cyclooxygenase-2 inhibitors in the management of tumor angiogenesis. *Prog Exp Tumor Res* 2003; **37**:179–192.

38 Oshima M, Taketo MM. COX selectivity and animal models for colon cancer. *Curr Pharm Des* 2002; **8**:1021–1034.